

A Novel Method of Hysteresis Direct Torque Control of Single-Phase Induction Motor Drives

Ahmed Alaa Mahfouz⁽¹⁾, Ashraf I. El- Nagga⁽²⁾, Anton S. Riad⁽²⁾

⁽¹⁾ *Cairo University, Faculty of Engineering, Electrical Power and Machines Department, Giza, Egypt.*

⁽²⁾ *Fayoum University, Faculty of Engineering, Electrical Engineering Department, Fayoum, Egypt.*

Email: aelkousy@yahoo.com

(Received 27/9/2013; accepted for publication 22/11/2013)

ABSTRACT. This paper investigates the principle of direct torque control when applied to single-phase induction motor drive. The presented direct torque control is based on hysteresis band strategy. The proposed control scheme utilizes voltage source inverter consisting of a single-phase rectifier cascaded with a four-switch inverter that provides nine voltage vectors and divided the dq plane into eight sectors. A modified switching pattern has been discussed to improve the performance of the drive. Simulation results have been provided to illustrate the system operation. A comparison between the presented scheme and another direct torque control drive scheme has been held.

Keywords: Direct torque control; single-phase induction motor; hysteresis comparator.

1. Introduction

Over many years, most of the high performance techniques of induction motor drives that are widely used in industry were restricted to three-phase machines. However, most of them can be modified in order to be valid for single-phase induction motor drives that are the most utilized machines in the domestic and fractional horsepower applications. Thus, a modern technique, direct torque and flux control (DTFC), that precisely controls this popular machine will be investigated in this paper.

In general, single-phase machine can be viewed as a two-phase machine (main and auxiliary windings), since these windings are orthogonal in space and usually have different impedances. The most common types of such motors are the split-phase, capacitor-start, capacitor-run and capacitor-start capacitor-run. These types may need mechanical centrifugal switches to cut out the startup capacitors. In the presented control technique, all of these capacitors and centrifugal switches will be removed.

Many papers have investigated different control techniques for single-phase induction motor drives. In [2] the capacitance (dc capacitor is inserted in series with the auxiliary winding of the single-phase machine) can be controlled by controlling the switching of a transistor H bridge in order improve the performance of the machine. The constant V/f strategy has been applied to control a four-switch inverter feeds the single-phase machine in [3]. Rotor-flux-oriented control of a single-phase induction motor drive has been presented in [4]. The disadvantage of such methods is their need to a speed encoder; hence, the costs will be high if it is compared with the price of the motor itself. Recently, Neves et al. [5] have presented direct torque control (DTC) technique to control single-phase machine drives that is a promising strategy. Neves has presented two methods of DTC; hysteresis DTC and Field oriented DTC. The switching pattern that is utilized in the hysteresis DTC drive presented in [5] provides four active switching states only. This pattern causes a problem when the stator flux vector is near the border of a sector; the voltage vector component in quadrature with the flux vector may be too small to give the desired result of reducing the torque error and the technique may fail.

In the present paper, a modified hysteresis DTC scheme with a modified voltage source inverter-switching pattern will be introduced. As in most DTC three-phase drives, current, speed, or position controllers are not necessary for the torque and flux control. Thus, a significant reduction in drive cost will be achieved.

The proposed VSI configuration shown in Figure (1) with the modified switching patters will provide eight active switching states (voltage vectors) and one zero-voltage vector; this will divide the dq plan into eight sectors.

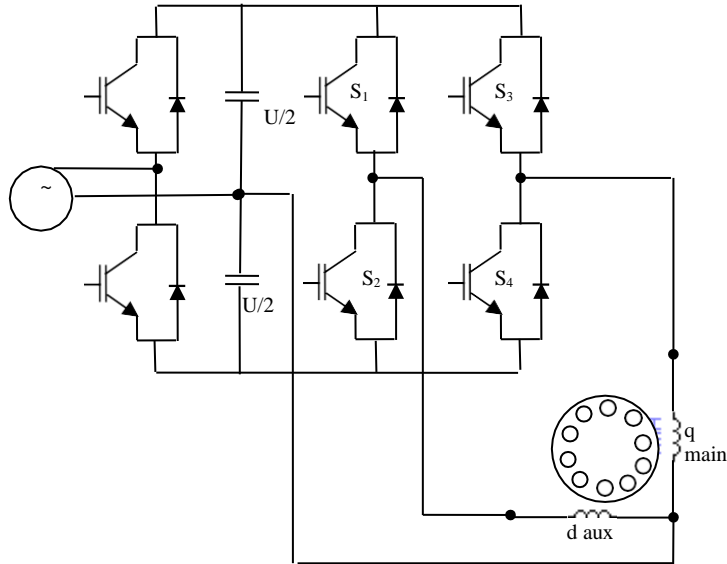


Fig. (1). Single-phase induction motor drive system.

2. Single-Phase Induction Machine Model

The mathematical model that describes the dynamic and the electric behaviors of single-phase induction motors can be summarized in the following equations:

$$v_{qs} = r_{qs} i_{qs} \quad \lambda'_{ds} = L_{qm} i_{qs} \quad (6)$$

$$v'_{ds} = r'_{ds} i'_{ds} \quad \lambda'_{qr} = L_r i'_{qr} \quad (7)$$

$$0 = r'_{qr} i'_{qr} + \frac{d\lambda'_{dr}}{dt} \quad \lambda'_{dr} = L_r i'_{dr} \quad (8)$$

$$0 = r'_{dr} i'_{dr} + \frac{d\lambda'_{qr}}{dt} \quad T_e = \frac{PL_q}{2I_r} - \lambda'_{dr} i'_{qr} \quad (9)$$

$$\lambda_{qs} = L_{qs} i_{qs} \quad \frac{P}{2} (T_e = \omega_r + \beta \omega_r) \quad (10)$$

where v_{qs} , v_{ds} , i_{qs} , i_{ds} , i_{qr} , i_{dr} , λ_{qs} , λ_{ds} , λ_{qr} and λ_{dr} are the dq-axes voltages, currents, and fluxes of the stator and rotor in the stator reference frame, r_{qs} , r_{ds} and r_r denote the stator and rotor resistances, L_{qs} , L_{ds} , L_r and L_{qm} denote the stator, and the rotor self- and mutual inductances, ω_r , T_e and T_L are the machine (electrical) speed, and the electromagnetic and load torque, and P , J and β are the machine poles, the inertia, and the viscous friction coefficient.

The primed symbols mean that their measured values are referred to stator q-axis quantities [1].

3. Direct Torque Control Principle

The instantaneous electromagnetic torque is proportional to the cross-product of the flux-linkage space vector and the stator-current space vector [6], [7]. This can be represented mathematically in equation (11)

$$T_e = C_1 \bar{\lambda}_s \times \bar{i}_s \quad (11)$$

Equation (11) can be rewritten in the following from:

$$T_e = C_2 |\bar{\lambda}_r| |\bar{\lambda}_s| \sin \gamma \quad (12)$$

Where \bar{i}_s , $\bar{\lambda}_s$, $\bar{\lambda}_r$ are the stator current space vector, stator and rotor flux-linkage space vectors, respectively, γ is the torque angle (the phase shift between the stator and rotor flux-linkage space vectors), C_1 , C_2 are constants that depend upon the machine parameters (*i.e.* number of poles, self and mutual inductances).

Equations (1) and (2) can be rewritten in a vector form as:

$$\bar{v}_s = r_s \bar{i}_s + d\bar{\lambda}_s / dt \quad (13)$$

Where $\bar{v}_s = v_{qs} + jv_{ds}$ is the stator voltage space vector. For simplicity, assume the stator ohmic drops to be neglected, then:

$$\bar{v}_s \approx d\bar{\lambda}_s / dt \quad (14)$$

or

$$\Delta\bar{\lambda}_s \approx \bar{v}_s \Delta t \quad (15)$$

It can be seen that the inverter output voltage directly impresses the stator flux, thus the required stator-flux locus will be obtained by using the appropriate inverter voltages (obtained by using the appropriate inverter switching states). It will be discussed below, how that comes true. It follows from Eqn. (15) that in a short time Δt , when the voltage vector is applied, $\Delta\bar{\lambda}_s \approx \bar{v}_s \Delta t$. Thus the stator flux-linkage space vector moves by $\Delta\bar{\lambda}_s$, in a trajectory parallel to the direction of the applied stator-voltage space vector (which is proportional to the D.C. link voltage).

The switching pattern that is utilized in the hysteresis DTC drive presented in [5] provides four active switching states only and causes a problem when the stator flux vector is near the border of a sector. The use of eight active voltage vectors will cure this problem by giving a chance of choosing a voltage vector for flux and torque correction that is around 45 degrees apart from the stator flux vector at the border of the sector.

The most important feature of the presented switching pattern is the redundancy of the voltage vectors; this greatly improves the performance; increases the torque response and reduce the torque and flux ripples, as it will be shown later [8], [9].

The VSI configuration shown in Fig.(1) can provide eight non-zero active voltage-switching vectors (\bar{u}_1 - \bar{u}_8) and one zero space vector \bar{u}_0 , as shown in Figure (2). As it is shown in Figure (1), each limb of the two-limb inverter has two power switches, each switch has two states (ON=1 or OFF=0). Hence, there are three possible switching modes; the three possible switching modes of the first limb for example are, $S_1=1$ and $S_2=0$, $S_1=0$ and $S_2=1$, or $S_1=0$ and $S_2=0$. Of course, the case at which both of the switches S_1 and S_2 are ON simultaneously is refused to avoid short circuit on the dc link to take place. Hence, the total possible switching states (voltage vectors) of the proposed inverter is $3^2=9$ states, where 3 is the number of the possible modes per limb and 2 is the number of limbs of the inverter. This VSI switching-pattern will divide the stator-voltage space into eight sectors; each sector covers forty-five electrical degrees.

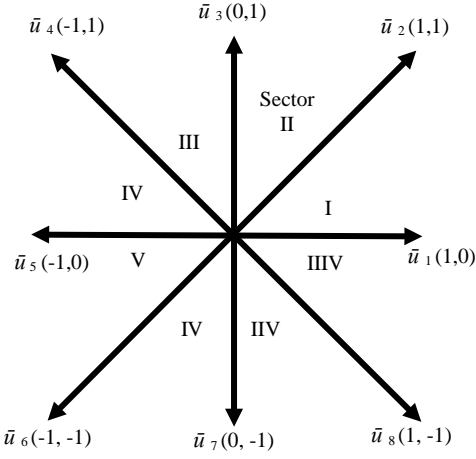


Fig. (2). Space vector plane of modified single-phase inverter.

The goal of the DTC principle is to control directly the magnitude of both of the developed torque and the stator flux linkage of the induction motor separately. It follows from (15) and Fig.(3) that \bar{v}_s^- can directly change both of the magnitude and the rotating speed of $\bar{\lambda}_s$. Torque control can be made easier by keeping the magnitude of $\bar{\lambda}_s$ constant in DTC, which in turn ensures that λ_r to remain constant as well. Therefore the motor instantaneous torque will directly change with the variation of the torque angle γ only, which is affected by the relative movement of $\bar{\lambda}_s$ and $\bar{\lambda}_r$. In Figure (3), if the magnitude of the measured stator flux linkage λ_s is greater than the given flux reference λ_s^* while it lays in sector 1, for instance, a voltage vector that forces λ_s to decrease is selected such as $\bar{u}_4, \bar{u}_5, \bar{u}_6$ or \bar{u}_7 . On the other hand, if λ_s is greater than λ_s^* , a voltage vector that impose λ_s to increase is exerted such as $\bar{u}_2, \bar{u}_3, \bar{u}_1$ or \bar{u}_8 . Using a similar manner in each sector ensures that the λ_s will be controlled within a pre-specified band.

4. Switching Lookup Table

In this section, the algorithm of selecting the voltage vector which controls both torque and flux simultaneously is described. Under the condition of flux magnitude being kept at a given value, according to Eqn. (12) the torque can be controlled by changing the torque angle γ . Suppose the rotor flux λ_r lags the stator flux λ_s by a

certain angle γ as depicted in Fig.(3). From Eqn. (15) it can be seen that γ is directly determined by the selected voltage vector. Hence rapid change in the developed torque can be obtained by altering the value of γ . Thus, if a torque increase is required, γ has to be enlarged and vice versa. Referring to the same example of which λ_s lays in sector 1 as seen in Figure (3), it can be seen that, applying u_2 or u_3 will result in enlarging γ while λ will be increased as will, u or u_4 enlarges γ and decreases λ , u_5 or u_1 reduces γ (λ will be forced to move towards λ_r) and increases λ_s and finally u_6 or u_7 reduces γ and decreases λ_s . Another method to decrease the torque (i.e. to reduce γ) is to apply a zero voltage vector; this will stop λ_s rotating while letting λ_r keep going.

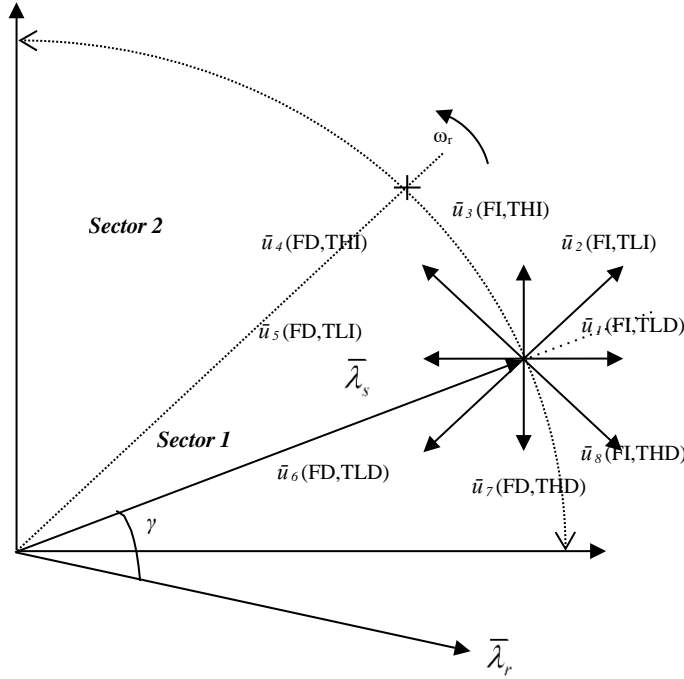


Fig. (3). Position of stator flux-linkage space-vector and selection of optimum switching voltage vector.

Figure (4) shows, according to the previous example, the effect of selecting two different voltage vectors on the torque angle. Suppose λ_{s0} is the flux-linkage vector which was originally located at P_0 , if it is required to increase the torque and

decrease the flux for instance, \bar{u}_4 or \bar{u}_5 will be adequate to be used; any of the new torque angles γ_2 or γ_1 will be greater than the original one γ_0 (*i.e.* torque increase will take place). But as γ_2 is greater than γ_1 , the rotating speed of γ in case of using \bar{u}_4 will be faster than that of its value in case of applying \bar{u}_5 for the same period of time. Thus, if a high torque response is required \bar{u}_4 will be efficient than \bar{u}_5 and vice versa. This can be seen clear in Fig. (3), where FI stands for flux increase; FD: flux decrease; THI: torque high increase; TLI: torque low increase; THD: torque high decrease and TLD: torque low decrease. In summary, by selecting the proper voltage vector both the flux and torque could be directly controlled at their given values. This can be summarized in a switching look-up table, as seen in Table (1).

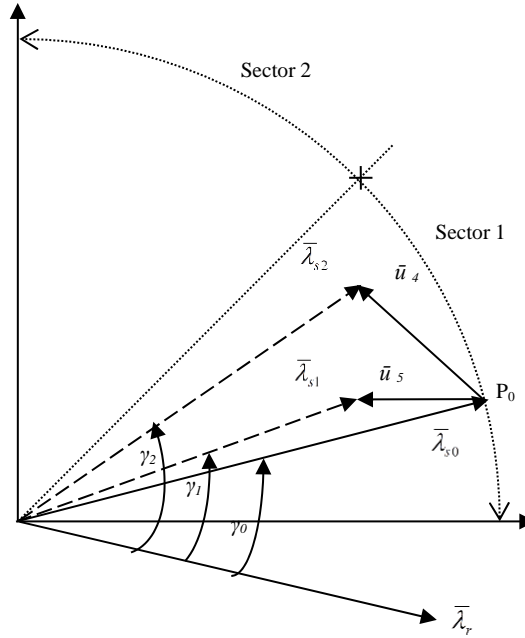


Fig. (4). Effect of the selected voltage vectors on advancing the angle of the stator flux-linkage space vector λ_s and torque angle γ .

Table (1). Optimal switching look-up table

$D\lambda$	dte	I	II	III	IV	V	VI	VII	VIII
1	-2	$\bar{u}8$	$\bar{u}1$	$\bar{u}2$	$\bar{u}3$	$\bar{u}4$	$\bar{u}5$	$\bar{u}6$	$\bar{u}7$
	-1	$\bar{u}1$	$\bar{u}2$	$\bar{u}3$	$\bar{u}4$	$\bar{u}5$	$\bar{u}6$	$\bar{u}7$	$\bar{u}8$
	0	$\bar{u}0$	$\bar{u}0$	$\bar{u}0$	$\bar{u}0$	$\bar{u}0$	$\bar{u}0$	$\bar{u}0$	$\bar{u}0$
	1	$\bar{u}2$	$\bar{u}3$	$\bar{u}4$	$\bar{u}5$	$\bar{u}6$	$\bar{u}7$	$\bar{u}8$	$\bar{u}1$
	2	$\bar{u}3$	$\bar{u}4$	$\bar{u}5$	$\bar{u}6$	$\bar{u}7$	$\bar{u}8$	$\bar{u}1$	$\bar{u}2$
0	-2	$\bar{u}7$	$\bar{u}8$	$\bar{u}1$	$\bar{u}2$	$\bar{u}3$	$\bar{u}4$	$\bar{u}5$	$\bar{u}6$
	-1	$\bar{u}6$	$\bar{u}7$	$\bar{u}8$	$\bar{u}1$	$\bar{u}2$	$\bar{u}3$	$\bar{u}4$	$\bar{u}5$
	0	$\bar{u}0$	$\bar{u}0$	$\bar{u}0$	$\bar{u}0$	$\bar{u}0$	$\bar{u}0$	$\bar{u}0$	$\bar{u}0$
	1	$\bar{u}5$	$\bar{u}6$	$\bar{u}7$	$\bar{u}8$	$\bar{u}1$	$\bar{u}2$	$\bar{u}3$	$\bar{u}4$
	2	$\bar{u}4$	$\bar{u}5$	$\bar{u}6$	$\bar{u}7$	$\bar{u}8$	$\bar{u}1$	$\bar{u}2$	$\bar{u}3$

5. Proposed DTC Scheme

Figure (5) shows the overall block diagram of the proposed direct torque control of single-phase induction motor drive. As shown in Figure (6-a), the flux comparator is a simple hysteresis comparator. If a stator flux-linkage increase is required then $d\lambda = 1$; if a stator flux-linkage decrease is required then $d\lambda = 0$. In the same manner for the torque comparator, as seen in Figure (6-b), If a high torque increase is required, then $dt_e = 2$. If a low torque increase is required, then $dt_e = 1$. If a high torque decrease is required, then $dt_e = -2$. If a low torque decrease is required, then $dt_e = -1$. If no change in the torque is required, then $dt_e = 0$.

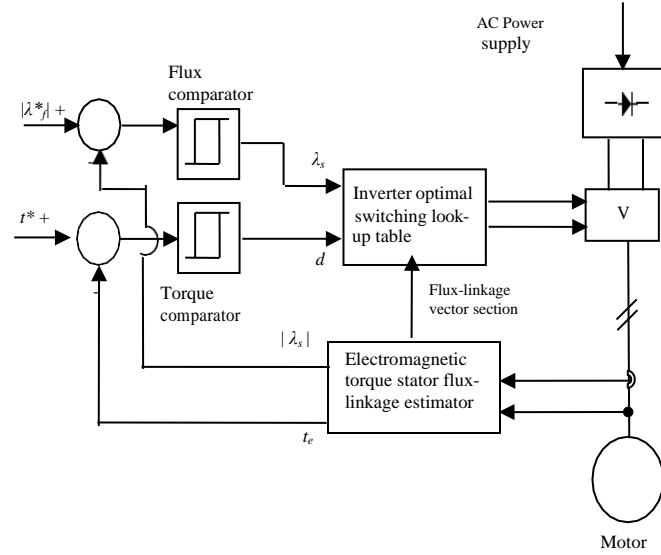


Fig. (5). Block schematic of direct torque and flux controlled single-phase induction motor drive.

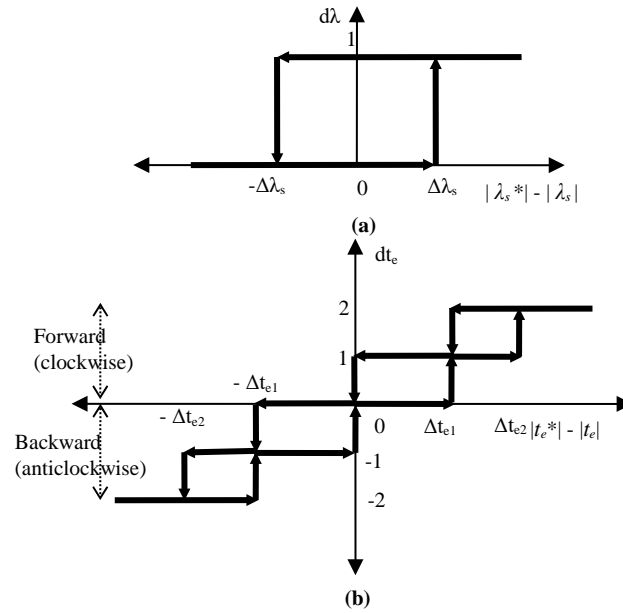


Fig. (6). Flux and Torque hysteresis loops, (a) Two-level (one loop) Flux hysteresis comparator, (b) Five-level (four-loop) Torque hysteresis comparator.

The optimum switching look-up table requires knowledge of the position of the stator flux-linkage space-vector. Since $\bar{\lambda}_s = |\bar{\lambda}_s| \exp(j\rho_s) = \lambda_{sq} + j\lambda_{sd}$, according to Figure (2), the location of $\bar{\lambda}_s$ can be determined according to the following algorithm:

if $\lambda_{sq} > 0$ and $\lambda_{sd} > 0$ then

if $|\lambda_{sq}| > |\lambda_{sd}|$ then $\alpha = \alpha(2)$ else $\alpha = \alpha(1)$

elseif $\lambda_{sq} > 0$ and $\lambda_{sd} < 0$ then

if $|\lambda_{sq}| > |\lambda_{sd}|$ then $\alpha = \alpha(7)$ else $\alpha = \alpha(8)$

elseif $\lambda_{sq} < 0$ and $\lambda_{sd} < 0$ then

if $|\lambda_{sq}| > |\lambda_{sd}|$ then $\alpha = \alpha(6)$ else $\alpha = \alpha(5)$

elseif $|\lambda_{sq}| > |\lambda_{sd}|$ then $\alpha = \alpha(3)$ else $\alpha = \alpha(4)$.

It is worthy to note that, the quadrature and direct components of the stator flux linkages λ_{sq} and λ_{sd} are estimated using equations (1) and (2):

$$\lambda_{sq} = \int (v_{sq} - r_{sq} i_{sq}) dt \quad (16)$$

$$\lambda_{sd} = \int (v_{sd} - r_{sd} i_{sd}) dt \quad (17)$$

6. Simulation Results

The performance of the drive system as regarding torque, flux, stator currents has been determined with the help of a simulation tool (Simulink 4.0, in Matlab 6.0 (R12), MathWorks, Inc.). The electrical and mechanical parameters of the single-phase induction motor that is used in the simulations are given in the appendix.

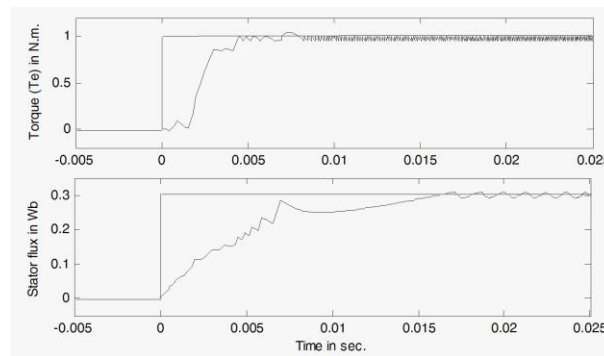


Fig.(7). Torque (N.m) and flux (Wb) responses of the proposed hysteresis DTC scheme at start-up.

Figure (7) shows the DTC drive response when the drive starts-up from rest (*i.e.* no initial magnetic flux) with a demanded load torque of 1N.m and settles within its pre-specified hysteresis band in 8 ms. In the same manner, stator flux was initially zero then rises to 0.3 Wb (reference value) within 16 ms. Figure (8) shows the stator currents at start-up. It can be seen from this figure that high current values reach about 300% are initially imposed in order to produce the magnetic flux. Such high currents disappear as soon as the flux reaches the reference value.

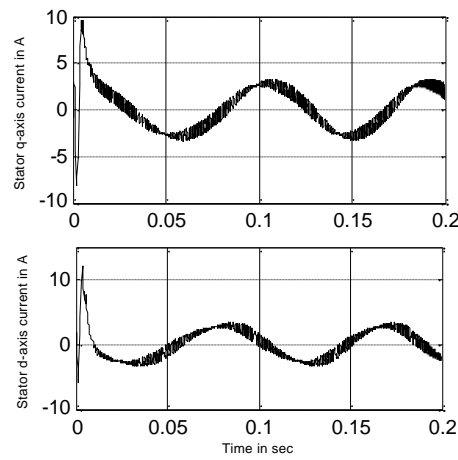


Fig. (8). Stator currents at start-up.

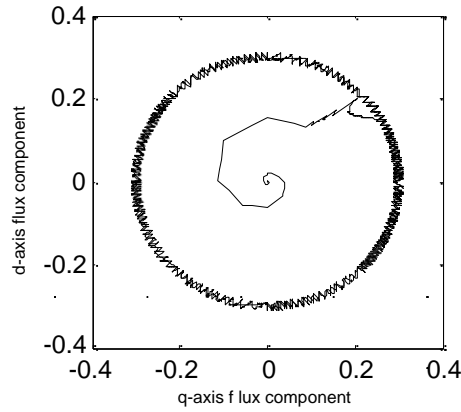


Fig. (9). Stator flux trajectory of DTC drive; its magnitude is set at 0.3 Wb.

Figure (9) shows the stator flux trajectory of the controlled motor using the DTC drive. It can be seen from that figure that the flux trajectory is a perfect circular path. This contrasts with the usual stator flux trajectory of single-phase induction motors which is usually sharp due to the windings asymmetry.

In Figure (10), the proposed DTC drive has been commanded to follow the torque reference at different operating points while flux reference is maintained at 0.4Wb. Torque commands of 0N.m, 1N.m, -1N.m and 0.5 N.m at $t = 0$ s, 0.2 s, 0.4 s, and 0.6 s, respectively, are applied. This figure shows the high torque response of the proposed DTC drive. Figure (11) shows the corresponding stator currents.

Figure (12) shows torque and flux zoom in around $t = 0.4$ s, it can be seen that, when the torque command has been changed from 1 N.m to -1 N.m, the electromagnetic torque follows the torque reference within about 250 μ s, while the stator flux has maintained within its hysteresis band (i.e. each of torque and flux is decoupled completely).

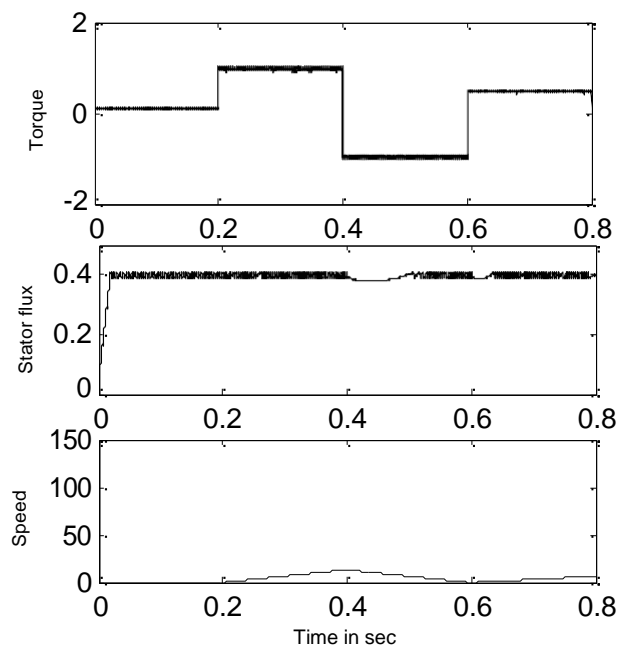


Fig. (10). Torque (N.m), Stator flux (Wb) and speed (rad/se).

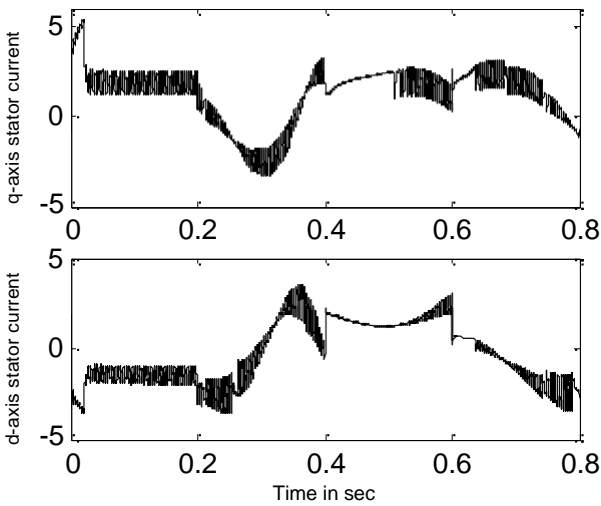


Fig. (11). Stator currents of the DTC drive in (A) during the different torque commands.

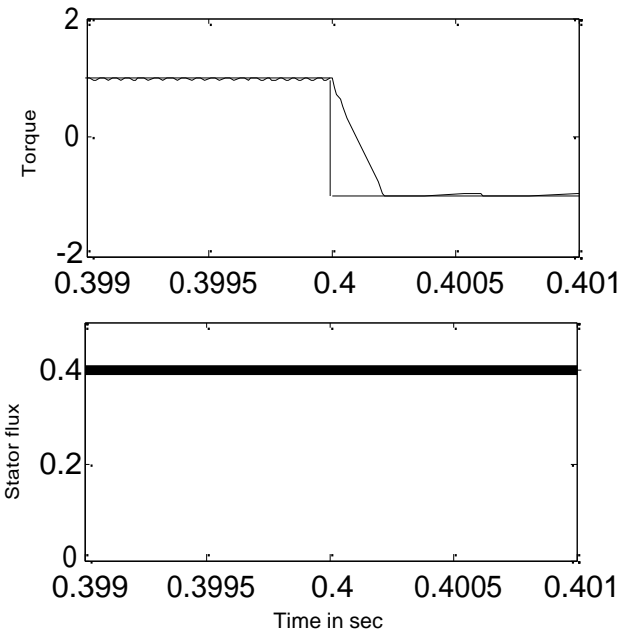


Fig. (12). Torque and flux zoom in at time $t = 0.4$ s.

For the purpose of comparing the response of the proposed DTC scheme with that has been presented in [4] at which another hysteresis DTC drive its VSI provides only four voltage vectors and divides the dq plan into four sectors only. Figure (13) is taken from [4] and shows the response of the DTC drive presented by Neves. It can be seen that, for the same torque and flux commands that were presented in Figure (10), in this figure, the torque ripples (noise) is greatly reduced from about 42 % of rated torque in case of Neves' model [4] to about 10 % in case of the present work due to the redundant stator-voltage space-vectors which can be provided by the VSI and PWM configuration.

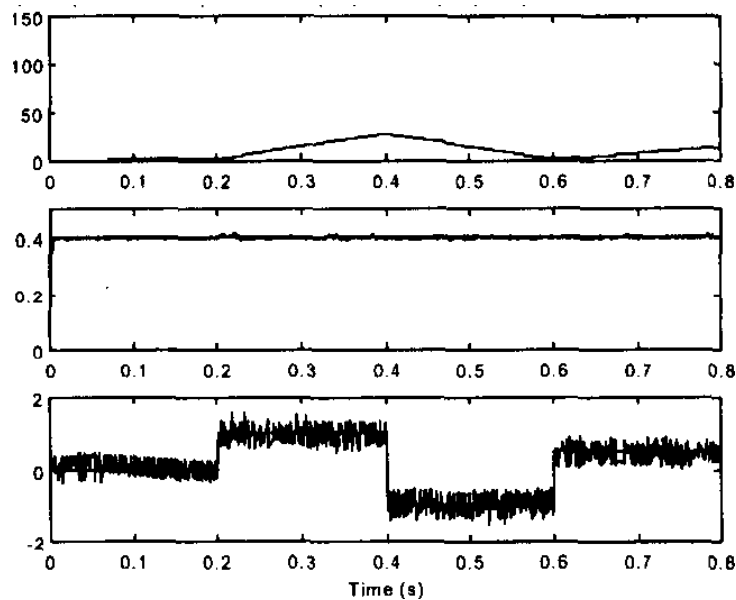


Fig. (13). Hysteresis DTC scheme presented by Neves [4]. Speed (elec. Rad/s), commanded and estimated stator and flux magnitude (Wb) and commanded and actual electromagnetic torque (N.m).

7. Conclusions

In this paper, a direct torque controlled drive of single-phase induction motors has been presented. The proposed scheme is based on the conventional hysteresis DTC schemes for three-phase induction motors. The proposed VSI configuration provides nine voltage-vectors and divides the dq plane into eight sectors. A switching lookup table is used to choose the optimal voltage-vector to control both of the stator flux-linkage and the torque separately. The proposed DTC algorithm distinguishes between low and high torque errors. The performance of the presented DTC scheme

has been tested by simulation. The simulation results shows fast torque and flux responses of this method. The eight-sector scheme presented in this paper, when compared with the four-sector scheme, reduces the torque noise from about 42 % to about 10 % of the rated torque. A problem associated with the four-sector scheme has been avoided.

8. References

- [1] Chee-Mun Ong, “*Dynamic Simulation of Electric Machinery, Using Matlab/Simulink*”, Prentice Hall PTR,(2006), pp. 214-221.
- [2] Lettenmaier, T. A., Novotny, D. W., and Lipo, T. A., “Single-Phase Induction Motor with an Electronically Controlled Capacitor”, *IEEE Transactions on Industrial Electronics*, vol. 27, no.1, (1991), pp. 38-43.
- [3] Corrêa, M. B. R., Jacobina, C. B., Lima, A. M. N., and Silva, E. R. C., “Rotor-Flux-Oriented Control of a Single-Phase Induction Motor Drive”, *IEEE Transactions on Industrial Electronics*, vol. 47, No.4, (2000), pp. 832-841.
- [4] Neves, F. A. S., Landim, R. P., Filho, E. B. S., Lins, Z. D., Cruz, J. M. S., and Accioly, A. G. H., “Single-Phase Induction Motor Drives with Direct Torque Control”, *28th Annual Conference of the IEEE Industrial Electronics Society (IECON)*, vol. 1, Nov. 5 to 8, (2002), pp. 241-246.
- [5] Takahashi, I., Noguchi, T., A new quick-response and high efficiency control strategy of an induction motor, *IEEE Transactions on Industry Applications*, vol. IA-22, no.5, (1986), pp. 820-827.
- [6] Takahashi, I., and Ohmori, Y., “High-Performance Direct Control of an Induction Motor”, *IEEE Transactions on Industry Applications*, vol. 25, No.2, (1989), pp. 257-264.
- [7] Vas, P., “*Sensorless Vector and Direct Torque Control*”, Chapter 4, Oxford University Press, (1998).
- [8] Young, C. M., Liu, C. C., and Liu, C. H., “New inverter-driven design and control method for two-phase induction motor drives”, *IEE Proceedings Electric Power Applications*, vol. 143, no. 6, (1996) , pp. 458-446.
- [9] El Badsì, B., Bouzidi, B., and Masmoudi, A., "DTC Scheme for a Four-Switch Inverter-Fed Induction Motor Emulating the Six-Switch Inverter Operation", *IEEE Transactions on Power Electronics*, vol. 28, No. 7, (2013), pp. 3528-3538.

نحاطة الوجه. و السلوب المستخدم مبني على اسرنا لوجبة الذي اق ايذا (hysteresis band). و يستخدم سربوب الماكلم ٥٥ حول جند العكس) Voltage Source Inverter (مكفو) نم مؤوم نينا نحااي الوجهه ماصل على الالوال) سبلول اباوع) المانلوح يغوي ايرك باسعة ماحدات جد و يؤسم تراغ dq (ل) ماببة اوسنام. كفا نناوش كل نونا ماقدم لرنا ناء ماعومة الحنا : نام انا انا ماحه املند المراسلم نم جند جدول الاقي نونا المؤندم. نممر نالوج عملية ايكاة با اسم الشخص) للشكل المؤدم , و سقا انا مابنا انا كل رخنر للماكللم بف العنم لذن الماعومة يؤسم تراغ dq (ل) نايعة اوسنام و يغوي ايرك باايعة ماحدات جند. نالاشنو بف عنم ايرك اكنض م 22%) مم الوبمة اللمسبة لعنم ايرك (لم بف الشكل ال انا) انا 11% بف الشكل المؤدم بف ٥٥ الموالفة. كفا مبالغلم على مشكلة كابت نواجه الشكل ال اخر نواجة لولة لعدا ماحدات املد.

